# Nucleation environment of diamonds from Yakutian kimberlite

**Article** *in* Mineralogical Magazine · June 1998

DOI: 10.1180/002646198547675

CITATIONS
82

READS
143

**3 authors**, including:

William L. Griffin
Macquarie University
**571** PUBLICATIONS **32,187** CITATIONS
SEE PROFILE

Chris Ryan
The Commonwealth Scientific and Industrial Research Organisation
**354** PUBLICATIONS **13,726** CITATIONS
SEE PROFILE

*Mineralogical Magazine, June 1998, Vol. 62(3), pp. 409–419*

# Nucleation environment of diamonds from Yakutian kimberlites

G. P. BULANOVA

TSNIGRI, Varshavsky sh. 129B, 113545 Moscow, Russia

W. L. GRIFFIN

GEMOC Key Centre, School of Earth Sciences, Macquarie University, Sydney 2109, Australia

AND

C. G. RYAN

CSIRO Exploration and Mining, Box 136, North Ryde 2113, Australia

**ABSTRACT**

The micro-inclusions located in the genetic centre of Yakutian diamond monocrystals have been studied using optical (anomalous birefringence, photoluminescence, cathodoluminescence) and microanalytical (electron-microprobe, proton-microprobe, scanning electron microscope) methods. Most diamonds nucleated heterogeneously on mineral seeds, that lowered the energy barrier to nucleation. Nucleation of peridotitic diamonds occurred on a matrix of graphite+iron+wüstite, in an environment dominated by forsteritic olivine and Fe-Ni sulfide. Nucleation of eclogitic diamonds occurred on a matrix of sulfide $\pm$ iron in an environment dominated by Fe-sulfide and omphacite ($\pm$K-Na-Al-Si-melt). The mineral assemblages recorded in the central inclusions of Yakutian diamonds indicate that they grew in a reduced environment, with oxygen fugacity controlled by the iron-wüstite equilibrium. Nucleation of diamond occurred in the presence of a fluid, possibly a volatile-rich silicate melt, highly enriched in LIL (K, Ba, Rb, Sr) and HFSE (Nb, Ti, Zr) elements. This fluid also carried immiscible Fe-Ni-sulfide melts, and possibly a carbonatitic component; the introduction of this fluid into a reduced refractory environment may have been accompanied by a thermal pulse, and may have created the conditions necessary for the nucleation and growth of diamond.

**KEYWORDS:** diamond, inclusions, nucleation, growth, Yakutia, kimberlite.

## Introduction

WHILE natural microdiamonds of different origin (metamorphic, impact, 'crustal') occur in many different geological settings, large ($\geqslant$2 mm) diamond monocrystals are found only in kimberlitic and lamproitic volcanic rocks. These diamonds appear to have formed at high pressure and temperature within their stability field, in either peridotitic or eclogitic environments, and to have been transported to the surface by the kimberlites and lamproites. Macrodiamonds from kimberlites give ancient (1.6–3.4 Ga) radiometric ages, may have complex histories of formation with multiple growth, dissolution and regrowth features; incorporate nitrogen, hydrogen and oxygen as impurities; and show evidence of different degrees of post-growth resorption. The problem of the origin of macrodiamonds in the Earth's upper mantle can be addressed through integrated studies of the internal morphology of the diamonds and the mineralogical and chemical environment in which they nucleated.

The nucleation point or 'genetic centre' from which an individual diamond has grown can be located using images of anomalous birefringence (ABR; Fig 1), UV photoluminescence (PL; Fig. 2) and cathodoluminescence (CL; Fig.3). The petrographic study of more than 10,000 octahedral macrodiamonds from Yakutian kimberlite pipes has shown the existence of microscopic inclusions in the genetic centre of the stone in 60% of the

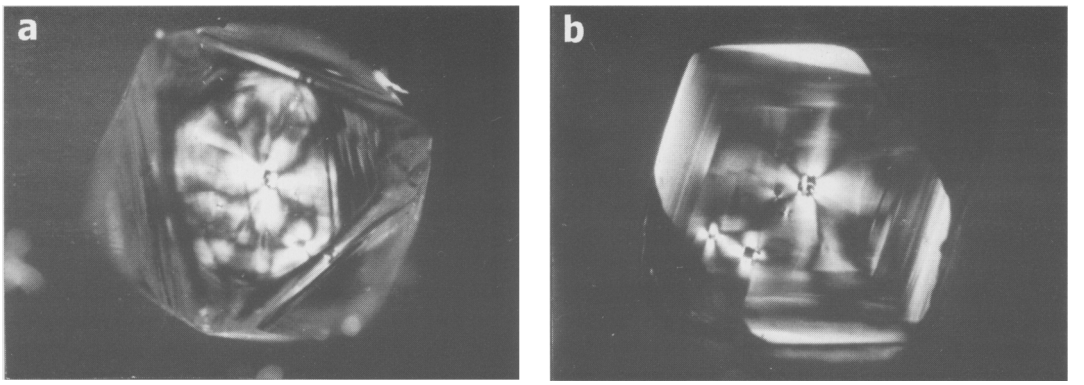


FIG. 1. (*a*) Sector-zoned internal structure of diamond shown by anomalous birefringence ; note group of central inclusions. (*b*) Plate of the same stone sawn on (110) plane showing central inclusions at the genetic centre. Width of diamond 5 mm.

population studied (Bulanova *et al.*, 1979). Nearly all stones in which the genetic centre can be clearly and unambiguously identified by ABR images contain such micro-inclusions, termed 'central' by Varshavskiy (1968). These inclusions very often mark the apices of dislocation bundles, suggesting that the diamond monocrystals have grown by a dislocation-controlled growth mechanism (Sunagawa, 1984). The inclusions typically are 1–15 μm in diameter, opaque and faceted; shapes include prisms, octahedra and thin triangular or hexagonal plates (Fig. 4). Thin, amoeboid opaque inclusions resemble the inclusions of metallic catalyst seen in synthetic diamonds (Fig. 4*c*).

The central inclusions may occur singly or in tight groups. Where only a single inclusion is present, it is invariably located in the genetic centre of the diamond (Figs 2,3), and thus appears to represent the nucleation point of the diamond. This will be referred to as the 'seed', without meaning to imply epitaxial growth of the diamond on the seed. Where there is a group of micro-inclusions in the centre of diamond, they tend to be arranged in a

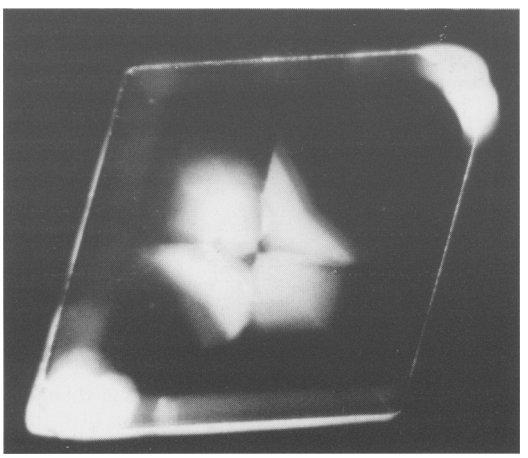

FIG. 2. Photo-luminescence image of (110) plate from specimen 3064 (width 3.5 mm). Note the sector-zoned structure of the 'central cross' (which shows yellow PL) and the cubo-octahedral shape of the central growth zone. Hydrogen occurs only within the 'central cross'; the 'seed' shown in Table 1 occurs at the centre of the cross and consists of monocrystalline graphite.

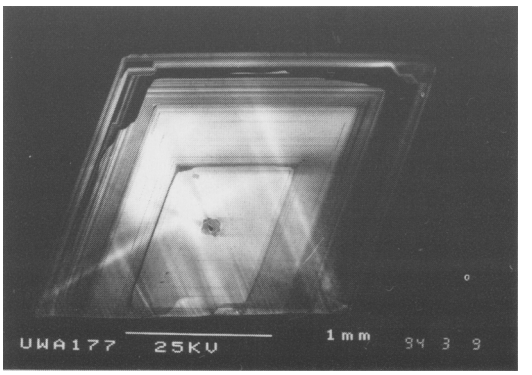


FIG. 3. CL-image of (110) plate of peridotitic diamond 3158, with inclusion of pyrope at the nucleation point. Width of crystal 3.7 mm.

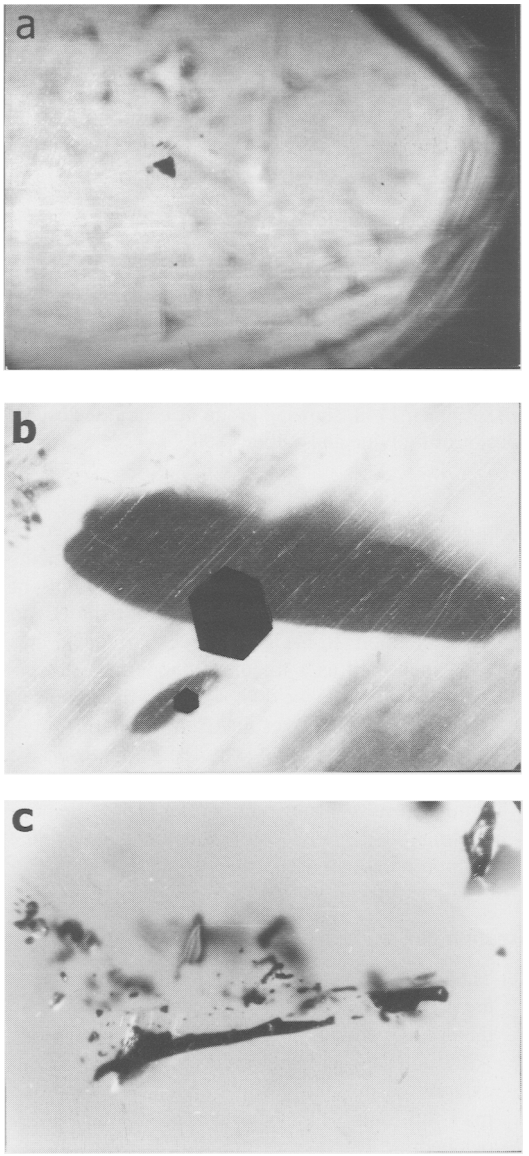


FIG. 4. Central inclusions of (*a*) triangular, (*b*) hexagonal and (*c*) irregular shape. Magnifications 150×, 1000× and 350×, respectively.

closely-spaced configuration about the genetic centre, so that no single inclusion clearly predates than the others (Figs 4,5). All of these inclusions appear to have been trapped during the very earliest stages of diamond growth, and thus provide unique information about the environment in which diamond monocrystals nucleated.

In this report we present new data on the composition of the central inclusions in several Yakutian diamonds, based on scanning electron microscopy (SEM) and proton microprobe (PMP) analysis, and discuss their implications for the environment and processes of diamond nucleation and growth.

## Methods and samples

We selected gem-quality octahedral diamond monocrystals (4–5 mm in size) that have distinctive internal structures, as shown by birefringence and UV photo-luminescence images, so that the genetic centre could be clearly identified. Stones were further selected to have central inclusions >5 μm in diameter. The diamonds were sawn on their rhombic dodecahedron plane, and polished to reveal the central inclusions. Several inclusions were left a few μm below the polished surface, where they could be studied by proton microprobe without risk of contamination. The inclusions have been studied optically in transmitted and reflected light, and those on the surface have been identified by use of a Camebax electron microprobe. In general, the small size of the inclusions and the multiphase nature of some (see below) hinder quantitative analysis. Carbon was identified by its $K\alpha$ line, using a thin-window spectrometer on the Camebax. Some inclusions were also studied by analytical SEM at the CSIRO Division of Coal and Energy Technology (North Ryde); both C and O could be identified with this instrument.

Bulk compositions (for elements heavier than Si) of the inclusions were measured using the proton microprobe at CSIRO Exploration and Mining, North Ryde. A beam of 3 MeV protons was focussed to a spot c. 15 μm in diameter; in most cases this is larger than the inclusions being analysed. X-rays generated by the proton beam were collected by a Si(Li) energy-dispersive detector, and the resulting X-ray spectra were treated as described by Ryan *et al.* (1991). Most inclusions were analysed using a 250 μm Be filter between the sample and the detector to attenuate the continuum background. This provides analyses for all elements heavier than Si, though the data are only semiquantitative for S. Some inclusions were also analysed using a 200 μm Al filter; this procedure precludes analysis of elements lighter than Fe, but allows higher beam currents and more precise analysis of heavy elements. The penetrating power of the proton

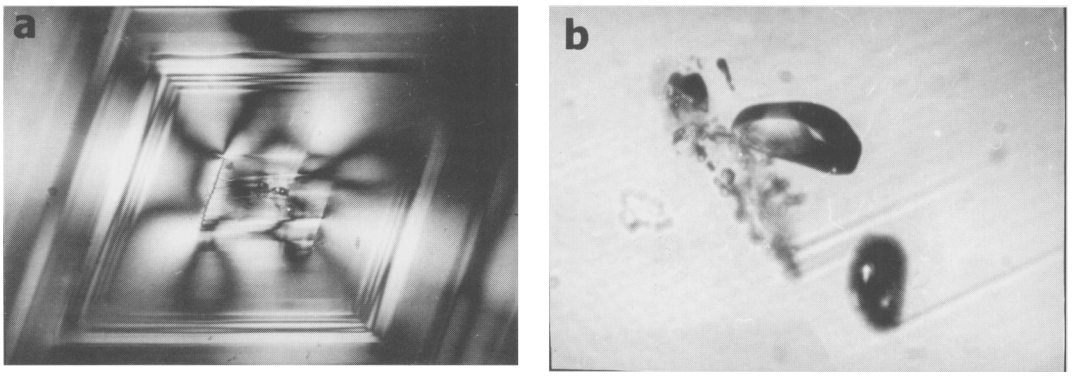


FIG. 5. (*a*) ABR image of octahedral central growth zoning in specimen 1142, showing group of central inclusions (magn. 15 ×, crossed nicols); (*b*) central inclusions of olivine and sulfide (300 ×).

microprobe also was used to analyse inclusions 3–6 μm below the surface of the polished plates. In this case the absorption of X-rays by the overlying diamond greatly reduces the peaks of the lighter elements, and changes their apparent relative abundances ( e.g. Cl/K and K/Ca ratios).

Because of the size of the proton beam and its penetrating power (to 35–50 μm), the inclusions analysed here represent only part of the volume analysed. This geometrical problem, and the heterogeneous nature of some individual inclusions, mean that the analyses reported here represent only semiquantitative estimates of the relative proportions of those elements in the bulk material of each inclusion. This is especially true of the analyses of subsurface inclusions. The emphasis in this report therefore is on the presence of significant elements and combinations of elements, rather than on their absolute abundances.

Some inclusions have been opened during polishing, and appear as faceted cavities on the polished diamond surface. Our experience with the mechanical polishing of diamonds shows that very complicated processes sometimes take place at the contact between the diamond and the cast-iron lap. Negative relief on the diamond surface may be filled with an alloy-like combination of iron and the polishing compounds, formed at the high temperature of the polishing process. This raises the possibility that the cavities could be filled with polishing material, especially Fe from the polishing lap, as they are opened. To avoid the identification of such filled negative cavities as natural materials, we have analysed (by proton microprobe) all materials, including Fe laps, polishing compounds, glues and resins, used in the polishing process. None of the elements reported below, with the possible exceptions of Cu, Zn, Fe and Cl, could be attributed to contamination from this source. Iron also has been identified as a major component in subsurface inclusions, so we do not believe that the Fe in exposed inclusions results from contamination. Finally, the analysis of exposed and subsurface micro-inclusions in single diamond gave very similar results (Table 1, N1558,3181), demonstrating the lack of contamination between the diamond and cast-iron lap.

## Results

The results of the analyses of the central inclusions are presented in Table 1. The central area of these diamonds commonly shows yellow PL and CL. Although all the diamonds have octahedral external forms, the shape of their central zones may be cubic, rounded, cubo-octahedral or octahedral. This shows that the diamond monocrystals have changed their form during growth from the nucleation stage to the larger crystal, probably in response to environmental changes (Sunagawa, 1984; Bulanova, 1995).

Inclusions identified in the central area of the diamonds can be divided into two groups. Group One consists of single inclusions or closely spaced clusters of inclusions 10–20 μm in diameter, grouped around the nucleation centre of the diamond. These inclusions are typically silicates or sulfides with compositions similar to those commonly associated with diamonds. In diamonds of the peridotitic paragenesis the most

TABLE 1. Data on diamonds and central inclusions

| Sample | 1565/1 | 1565/2 | 3615 | 1142 | 1516/2 | 1558/1 | 1558/2 | 1558/3 | 3181/1 | 3181/2 |
|---|---|---|---|---|---|---|---|---|---|---|
| Locality | Mir | Mir | Udachnaya | Mir | Mir | Mir | Mir | Mir | Udachnaya | Udachnaya |
| Paragenesis | peridotitic | peridotitic | peridotitic | peridotitic | peridotitic | peridotitic | peridotitic | peridotitic | peridotitic | peridotitic |
| Core PL colour | yellow | yellow | blue-green | yellow | blue | blue | blue | blue | blue | blue |
| Core shape | cubo-oct. | cubo-oct. | octahedral | rounded | cubo-octa. | octahedral | octahedral | octahedral | octahedral | octahedral |
| Grp 1 inc. | Oliv $Fo_{92}$ | Oliv $Fo_{92}$ | Oliv+Chrom. | $Fo_{93}$+sulf | $Fo_{93}$ | oliv+ sulf | oliv+ sulf | oliv+ sulf | chromite | chromite |
| Grp 2 inc.* | Grph+sulf+Fe | Grph+sulf+Fe | black microin. | | Grph | Grph | Grph | Grph | black microin. | |
| Analysed incl. | 'seed' | 'seed' | 'seed' | ol+sulf | 'seed' | 'seed' | 'seed' | 'seed' | plate | plate |
| Location | open | open | subsurface | subsurface | on surface | on surface | subsurface | subsurface | subsurface | subsurface |
| Filter | Be+Al | Be+Al | Be | Be | Be | Be | Be | Be | Be | Be |
| Si | <70 | 300 | 650 | <200 | | | | | | |
| S | <6 | 75±11 | 580±50 | 0.75% | | | | | | |
| Cl | 101±7 | 45±5 | 920±50 | <20 | 6±3 | <14 | <7 | <5 | | |
| K | 1970±50 | 145±5 | 330±12 | <7 | 47±2 | 87±3 | 117±5 | 199±7 | <3 | <3 |
| Ca | 315±20 | 97±3 | 180±20 | 30±5 | 229±6 | 17±2 | 20±1 | 51±2 | 5.5±1 | 6±1 |
| Ti | 62±10 | 2±1 | 22±2 | <5 | 9±0.5 | 5±2 | 2.9±0.6 | 3±0.5 | 3±0.5 | 2±1 |
| Cr | 26±2 | 1.2±0.2 | 3±0.5 | <2.5 | 1.4±0.3 | 3.5±0.8 | 11±0.5 | 12±0.4 | 1±0.3 | 1.3±0.4 |
| Mn | 37±2 | 2±0.2 | 3±0.5 | <2 | <0.5 | <1 | 3±0.3 | 3.8±0.3 | 1.1±0.4 | 0.8±0.3 |
| Fe | 4900±200 | 1500±250 | 78±2 | 1% | 93±1 | 305±3 | 238±2 | 153±1 | 1±0.4 | 1.8±0.3 |
| Ni | 170±20 | 20±2 | 41±1 | 1.60% | 1.2±0.2 | <1 | 14±0.5 | 3.6±0.2 | 5.3±0.4 | 5.3±0.4 |
| Cu | 380±50 | 14±2 | 10±0.5 | 0.20% | 0.8±0.1 | 2.4±0.4 | <0.6 | <0.5 | <0.8 | <0.5 |
| Zn | 50±5 | 5±1 | 13±0.5 | <4 | 0.6±0.2 | <1 | 0.9±0.2 | 0.7±0.2 | <0.7 | <0.5 |
| Rb | 100±11 | <1 | 1±0.4 | | <0.5 | <1 | <1 | 0.7±0.2 | <0.8 | <0.6 |
| Sr | 270±18 | 5±1 | <1 | | 3.5±0.5 | <1.4 | 1.8±0.3 | 4.7±0.5 | <0.8 | <0.8 |
| Y | <4 | <1 | <1 | | <0.8 | <1.6 | <1 | <0.8 | <1 | <1 |
| Zr | 11±2 | <1 | <1 | | 1.5±0.5 | <2 | <1 | <1 | <1.3 | <1.2 |
| Nb | 240±12 | 6.5±1 | <1.5 | | <1 | | <1.3 | | | |
| Ba | 3110±400 | <30 | <50 | | <33 | | 39±19 | | | |
| La | <90 | | | | | | | | | |
| Ce | <100 | | | | | | | | | |
| Th | 13± | | | | | | | | | |
| Pb | <7 | | | | 1.6±0.5 | <2.3 | <4 | <1 | | |

(Continued on next page)

TABLE 1 (*contd.*)

| Sample | 3181/3 | 3181/4 | 1011 | 1584/1** | 3064 | 1137/1 | 1173/1 | 1545/1 | 1545/2 |
|---|---|---|---|---|---|---|---|---|---|
| Locality | Udachnaya | Udachnaya | Mir | Mir | Udachnaya | Mir | Mir | Mir | Mir |
| Paragenesis | peridotitic | peridotitic | eclogitic | eclogitic | unknown | unknown | unknown | unknown | unknown |
| Core PL colour | blue | blue | yellow | blue-green | yellow | yellow | yellow | blue | blue |
| Core shape | octahedral | octahedral | octahedral | rounded | cubic | cubo-octah. | cubo-octah. | octahedral | octahedral |
| Grp 1 inc. | chromite | chromite | | carbonate | | | | | |
| Grp 2 inc.* | | | black microin. | | Grph+Fe | Grph | Black plate | Grph+carb | Grph+carb |
| Analysed incl. | 'seed' | plate | 'seed' | carbonate | 'seed' | 'seed' | 'seed' | plate | carbonate |
| Location | on/under surf. | subsurface | open | on surface | subsurface | subsurface | on surface | subsurface | on surface |
| Filter | Be | Be | Be+Al | Al | Be | Be | Be | Be | Be |
| S | | | 1% | | 800 | | | <200 | 2.60% |
| S | | | <20 | | 150 | | | <25 | <25 |
| Cl | | | 60±20 | | 290±15 | <8 | 83±13 | 50 | 70±10 |
| K | 317±11 | <3 | 2830±65 | | 75±5 | 641±21 | 1010±33 | 75±7 | 190±10 |
| Ca | 56±4 | 5±1 | 615±60 | | 155±10 | 26±4 | 56±5 | 80±10 | 235±20 |
| Ti | 6±1 | 3±0.5 | 810±13 | | 28±2 | 4.5±0.8 | 42±8 | 9±1 | 9±3 |
| Cr | 2.8±0.5 | 0.9±0.4 | 4±0.5 | | 2±0.6 | 2.5±0.6 | 13±2 | 2±0.5 | 450±11 |
| Mn | 1.4±0.3 | 1±0.4 | 2.5±0.5 | 0.22% | <1 | 1±0.4 | 3.4±0.4 | <1 | 395±15 |
| Fe | 55±1 | 0.9±0.3 | 500±5 | 2.80% | 40±1 | 35±1 | 112±2 | 23±1 | 3.10% |
| Ni | 3.5±0.3 | 5.7±0.5 | 2.5±0.5 | 17±4 | 2±0.5 | 30±0.5 | 2.6±0.4 | 2±0.3 | 0.21% |
| Cu | <0.7 | <0.6 | 102±2 | 18±3 | 5±0.5 | <0.7 | 1±0.4 | 2±0.2 | <3 |
| Zn | 0.8±0.3 | <0.5 | 109±2 | 630±45 | 14±0.5 | <0.7 | <0.8 | <0.6 | <3 |
| Rb | <0.7 | <0.6 | 2.5±0.5 | 140±15 | <1 | 1.5±0.6 | 3.2±0.6 | 1±0.3 | |
| Sr | 13±1 | <0.7 | 26±1 | 0.69% | <1 | 1.5±0.5 | 46±2 | 1.2±0.3 | |
| Y | <1 | <1 | 4±0.5 | 100±5 | <1 | <1 | <1.5 | <1 | |
| Zr | <1.2 | <1 | 13±1 | 360±15 | <1 | <1.2 | <1.7 | <1.3 | |
| Nb | | | <2 | 290±7 | <1.5 | | | <1.5 | |
| Ba | <82 | | <60 | 0.25% | <40 | <84 | <84 | <60 | |
| La | | | na | 530±60 | | | | | |
| Ce | | | na | 980±85 | | | | | |
| Th | | | na | 60±7 | | | | | |
| Pb | <1 | | na | 0.10% | | | <1.7 | | |

*discrete phases identified by EMP, as or within 'central inclusions'

common central inclusion is olivine ($Fo_{92.5}$–$Fo_{93.6}$). More rarely, such inclusions may consist of another diamond, or of chromite; one example each of enstatite and lherzolitic garnet have been identified. These minerals are accompanied by pentlandite, or by monosulfide solid solution (MSS) enriched in Ni (Bulanova *et al.*, 1996).

In diamonds of eclogitic paragenesis, pyrrhotite (Po) and omphacite (mg# = 73.6–74.5; 100Ca/(Ca+Mg) = 49.4–52; %Jadeite = 48–54) are most common as central inclusions, and rare examples of pyrope-almandine garnet and coesite have been found. Silicate 'melt' micro-inclusions consisting of a K-Al-Si phase or having more complicated compositions sometimes are found in close association with central inclusions of omphacite (Bulanova *et al.*, 1988).

The second group of inclusions (Group Two, 'seeds') is represented by several opaque minerals, whose paragenesis (peridotitic or eclogitic) is less clear. They reach only a few μm in size and are located in the centres of diamond growth as single inclusions or tight groups of micro-inclusions. They appear most commonly as triangular or hexagonal plates, but some have no distinctive habit (Fig. 4*c*). These inclusions may consist either of single phases or of an heterogeneous mixture of phases. Detailed EMP/SEM studies of micro-inclusions in diamonds of the peridotitic paragenesis have identified: wüstite, graphite, sulfide, carbonate(?); monocrystalline graphite+native iron, taenite+sulfide, graphite+native iron+cohenite (Bulanova *et. al.*, 1979; Bulanova and Zayakina, 1991). In the eclogitic diamonds, Po and an unidentified K-Na-Al-Si phase were found (Bulanova *et al.*, 1988).

Group 2 micro-inclusions from seven peridotitic diamonds, two eclogitic diamonds and several diamonds of uncertain paragenesis were studied by PMP analysis (Table 2).

One of the Group 2 inclusions from peridotitic diamond 1565 (Table 1) was studied in detail by analytical SEM. An EMP analysis gave the following bulk composition: 2.63% $SiO_2$; 55.9% FeO; 5.1% MgO; 1.9% CaO; 2.7% $K_2O$; 0.1% $Na_2O$; (+Ba, P, Cl as traces). This inclusion is made up of an heterogeneous distribution of phases, with no apparent zoning or regularity of distribution in the inclusion (Fig. 6), and the internal structure of the inclusion is very similar to a breccia. Analysis of apparently homogeneous subareas of the inclusion identified native iron, wüstite and graphite. In the areas of native iron and wüstite, small contents of Si, Mg and Al were recorded. In the areas consisting only of graphite K, Ca, Mg and Al were present.

Proton microprobe analysis of the same inclusion confirmed that Fe is the main heavy element present; Cl, K, Ca, Ni, Cu, Zn are also present, as well as a range of incompatible elements (Ti, Rb, Sr, Zr, Nb, Ba). While some of the observed elements (Fe, Cu, Zn, Cl) were detected in our study of the different polishing wheels and compounds, the large range of incompatible elements was not. We therefore consider that at least K, Ca, Ti and Ni have been present in significant amounts during the nucleation of the diamond and Rb, Sr, Zr, Nb and Ba in lesser amounts.

Proton microprobe analysis of other Group 2 inclusions in peridotitic diamonds, both exposed and subsurface (Table 1) confirms these observations, indicating that significant amounts of Cl, K, Ca, Ti, Fe, Ni, Cu and Zn are present in subsurface inclusions, where there is no possibility of contamination during polishing. The observation of the S-$K\alpha$ line in the spectrum from the micro-inclusion in sample 3615, despite the presence of an overlying 'lid' of diamond, indicates a significant sulfide component. Several opaque plates in peridotitic diamond 3181 contain much more Ni than Fe, together with low levels of other elements; the nature of this phase is unknown, but it appears to be native Ni. Similar plates have been observed by us in other Udachnaya diamonds, but not as central inclusions.

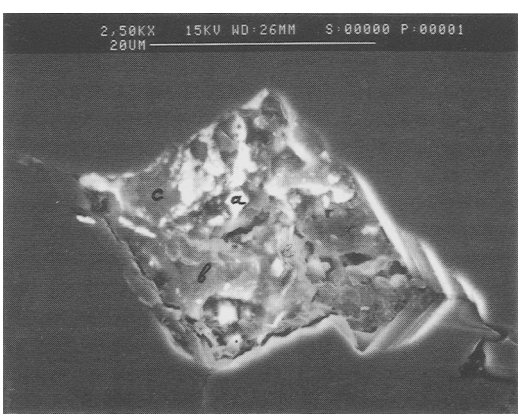


FIG. 6. SEM image of heterogeneous central inclusion exposed on plate from specimen 1565. a, native Fe; b, wüstite; c, graphite. Long axis of inclusion is 25 μm.

TABLE 2. Trace element analyses of diamonds

| Locality | Argyle | Argyle | Kimberley, SA | Finsch | Finsch | Finsch | Zaire | Jwaneng |
|---|---|---|---|---|---|---|---|---|
| Sample | macrodiam. | gems | gems | incl-free | with incl. | with incl. | cubes | cubes |
| No. analysed | n = 10 | n = 18 | n = 34 | *c.* 250 | *c.* 350 | 1 (10 cuts) | n = 5 | n = 4 |
| Technique* | PMP | PMP | PMP | NAA | NAA | NAA | PMP | PMP |
| Reference | 1 | 1 | 1 | 2 | 2 | 3 | 1 | 1,4 |
| Type Comp.** | Sum spectrum | Sum spectrum | mean | mean | mean | mean | Sum spectrum | Fluid |
| S | 36±4 | 120±10 | n.a. | b.d. | 10 | n.a. | 22±3 | |
| Cl | 17±2 | 40±3 | 250±400 | 0.067 | 0.6 | n.a. | 16±1.5 | 4.50% |
| K | 76±1 | 9.7±0.3 | 20±35 | 0.18 | 2.7 | 2±0.7 | 103±2 | 15.50% |
| Ca | 72±1 | 21.7±0.6 | 40±35 | 1.02 | 2.7 | n.a. | 74±1 | 7.00% |
| Ti | 16±1 | 1.4±0.1 | 0.5±0.5 | 0.05 | 0.26 | n.a. | 15±1 | 2.60% |
| Cr | <0.6 | <0.1 | 0.4±0.5 | 0.04 | 2.1 | 0.43±0.55 | <0.2 | bd |
| Mn | 0.9±0.2 | <0.1 | n.a. | 0.01 | 0.31 | 79±108 | 0.7±0.1 | bd |
| Fe | 190±1 | 24.5±0.3 | 10±10 | 0.61 | 15 | 25±24 | 66±1 | 10.90% |
| Ni | <0.5 | 0.8±0.1 | 1±1 | 0.37 | 5.5 | 1.8±1.5 | 0.5±0.05 | 1345 |
| Cu | 2.6±0.2 | 1.1±0.1 | 1.5±1 | 0.34 | 0.71 | n.a. | 12.5±0.1 | bd |
| Zn | 1.3±0.1 | 0.9±0.1 | 1.5±1.5 | n.a. | n.a. | n.a. | 1.3±0.1 | 2000 |
| Rb | 7.3±0.7 | <0.1 | | 0.015 | 0.023 | 0.03±0.02 | 0.5±0.1 | 730 |
| Sr | 1.9±0.5 | <0.2 | | 0.015 | 0.28 | n.a. | 7.7±0.3 | 3575 |
| Y | <2 | <0.2 | | n.a. | n.a. | n.a. | <0.4 | bd |
| Zr | 6.5±0.8 | 0.9±0.1 | | n.a. | n.a. | n.a. | 1.1±0.2 | 1920 |
| Ba | 120±30 | <11 | | 0.07 | 1.1 | 4.4±2.4 | 25±9 | bd |
| La | | | | 0.003 | 0.017 | 0.0±0..02 | | |

PMP= Proton microprobe; NAA= Neutron Activation Analysis
Uncertainties given as 1 std. dev.
n.a. not analysed; b.d. below detection level
**PMP data for Cl, K, Ti, Ni, Zn, Rb, Sr, Zr normalized to EMP Fe values
References: 1. Griffin and Ryan, unpubl. data; 2. Erasmus *et al.* (1977); 3. Bibby (1979); sequential dissolution of one stone; 4. Navon *et al.* (1993)

The analysis of one opaque plate identified by EMP as graphite also shows significant amounts of K, Ca, Ti, and Fe (1545/1; Table 1). Another inclusion in the same diamond (1545/2) gives an EMP analysis: 27% MgO, 5% FeO and admixtures of Ca, Na, K and Si, and is believed to consist mainly of a carbonate. The proton-probe spectrum of it (where Mg cannot be analysed) is dominated by Fe and Si, and also shows significant amounts of Cl, K, Ca, Cr and Mn.

A composite, partly exposed inclusion of olivine and sulfide (1142) also shows high levels of S, Fe and Ni; the dominance of Ni over Fe suggests that the sulfide is unusually Ni-rich. The spectrum of this inclusion, like those of other olivine inclusions analysed *in situ* by the proton microprobe, shows significant Ca; this is not observed in large olivine inclusions extracted from their diamonds, but has been observed in small inclusions where the surface material is included in the analysed volume (Griffin *et al.*, 1992, 1993). This observation suggests that the Ca is concentrated in a grain-boundary phase.

A central inclusion analysed in eclogitic diamond 1011 is enriched in Ti, Ca, Cu, Zn, Y, Zr and depleted in Ni, compared with the level of these elements in the central inclusions of peridotitic diamonds (Table 1).

After the analysis of the subsurface inclusions by the proton probe, we observed that extensive cracking of the diamond around the inclusions had taken place. This was not observed during the analysis of ordinary mineral inclusions. We also found that many central inclusions of Group 2 exploded before the diamond could be polished all the way down to the inclusion. These observations may provide indirect evidence for

the presence of a fluid component in the central inclusions of Group 2.

## Discussion

The central inclusions of Group 1 probably represent phases crystallized prior to, or simultaneously with, the nucleation of diamond and trapped as growth began. The inclusions of Group 2 appear, from their position at the genetic centre of the diamond, to be the seeds on which nucleation started, and their composition and commonly multiphase nature suggests that heterogeneous nucleation was involved. These fine-grained materials may have provided surface energy that could lower the energy barrier to the nucleation of diamond. The SEM observations on the seed of peridotitic diamond 1565 (Fig. 6), and the low concentrations of major elements even in exposed inclusions, suggest that the bulk of each seed in these diamonds consists mainly of graphite. We infer that this graphite formed before the diamond, probably metastably, and was the substrate on which diamond crystallized.

In a theoretical study of low-pressure chemical vapour deposition of diamond, Lambrecht *et al.* (1993) concluded that graphite is the first phase to form, and that diamond nucleation occurs in conjunction with hydrogenation of prism planes along the edges of graphite flakes. Infrared absorption studies of Yakutian diamonds show that hydrogen is typically present in the central zones of both peridotitic and eclogitic diamonds, but not in the intermediate or outer zones (Milledge *et al.*, 1993; Bulanova, 1995). The combination of monocrystalline graphite in the central inclusions and abundant hydrogen in the central zones of the diamonds, suggests that mechanisms similar to those proposed by Lambrecht *et al.* (1993) could be important in the nucleation of natural macrodiamond, at pressures and temperatures within its stability field.

The complete assemblage of minerals represented in the Group 2 central inclusions of peridotitic diamonds, and which may have acted as seeds and/or catalysts, is Ni-sulfide + native Fe (±Ni) + wüstite + monocrystalline graphite (±carbonate?). The oxide-sulfide-metal assemblage indicates that the redox conditions of diamond nucleation corresponded to the iron-wüstite buffer. The possible presence of carbonate in some inclusions, however, may suggest conditions closer to the wüstite-magnetite buffer.

The large contents of elements such as Cl, K, Ca, Ti, Rb, Sr, Zr, Nb and Ba in the central inclusions of octahedral peridotitic diamonds indicates that these diamonds have nucleated in an environment rich in incompatible large-ion lithophile (LIL) and high-field-strength elements (HFSE). This finding is remarkable; the overall chemical environment of such diamonds, as reflected in silicate and oxide inclusions, is characterized by extreme depletion in Ca and Al, so that most peridotitic diamonds contain harzburgitic rather than lherzolitic mineral inclusions (Meyer, 1987). Proton-microprobe studies of the trace-element contents of such syngenetic inclusions have confirmed that they also are depleted in LIL and HFSE elements, such as Rb, Ga, Y, Zr and Ti (Griffin *et al.*, 1992, 1993). However, anomalous second-stage enrichment in Sr and light rare-earth elements (*LREE*) has been recorded in harzburgitic chrome-pyrope garnet inclusions, and ascribed to a post-depletion metasomatic event preceding or accompanying the nucleation of diamond (Richardson *et al.*, 1984). Griffin *et al.* (1992) suggested that this event involved a carbonatitic fluid, high in Sr, Nb, Ba and *LREE*. The first direct identification of fluid microinclusions in peridotitic Siberian diamond (Schrauder *et al.*, 1993) shows they are rich in water, K, Cl and Sr-Ba-carbonates. This is strong evidence supporting the suggestion that metasomatic events in refractory environments are important to the nucleation and growth of diamonds.

The minerals occurring as Group 2 inclusions (seeds) in eclogitic diamonds are low-Ni MSS (monosulfide solid solution) or Po and a K-Na-Al-Si phase (melt?). The high content of elements such as K, Ca, Zn, Ti, Y and in lesser amounts Zr, Sr, Rb indicates that the nucleation of eclogitic diamonds, like that of peridotitic diamonds, took place in an environment rich in incompatible elements. The fluid that carried these incompatible elements may have been similar to the apparently syngenetic 'carbonate' inclusion analysed in diamond 1584 (Table 1), although this diamond is eclogitic rather than peridotitic. *In-situ* analyses of olivine, spinel and sulfide inclusions in diamonds, carried out during these investigations, have shown the presence of Ca, apparently concentrated at the interface between the inclusion and the host diamond (Bulanova, Griffin and Ryan, unpubl. data). We interpret this Ca as being present in a grain-boundary film between the olivine and the diamond, and suggest

that this film may consist of carbonate similar to that in inclusion 1584.

Analyses of trace elements in diamonds provide further evidence for the nature of the medium in which the diamonds grew. Table 2 shows representative trace-element data from several diamond populations. Proton-probe analyses of both peridotitic and eclogitic diamonds show high levels of Cl, K, Ca, Ti, Fe, Zn, Cu and Ni; other elements such as Rb, Sr, Zr and Ba appear in some spectra. This same suite of elements, as well as *REE* (strongly *LREE* enriched) has been found by NAA analysis of composite samples of diamonds from the Finsch kimberlite (believed to be largely peridotitic (Erasmus *et al.*, 1977)). Bibby (1979) used sequential dissolution to analyse the zonal distribution of trace elements in a Premier diamond with an inferred Cr-diopside inclusion, and found similar abundances of several elements (Table 2). Erasmus *et al.* (1977) concluded that these trace elements reside in submicroscopic inclusions of the fluid (*sl.*) phase from which the diamonds grew.

Studies of larger fluid (melt $\pm$ vapour $\pm$ daughter phases) inclusions in cubic diamonds have shown that these diamonds grew from K, Ca-rich fluids, which were probably volatile-rich silicate melts (Navon *et al.*, 1988; Schrauder and Navon, 1994; Schrauder *et al.*, 1996) and studies of similar samples by proton microprobe show that some of these fluids also contain significant levels of Cl, Rb and Sr (Griffin and Navon, unpubl. data). The similarities between the trace-element inventories of diamonds and those of the 'seeds' analysed here suggest that similar fluids and solid phases were present both during the nucleation and throughout the growth of many diamonds. The trapped material in these diamonds may represent a heterogeneous mixture of several end members, including iron and iron oxide, sulfide, carbonate and a fluid phase rich in K and Cl.

The most common phase in the central inclusions of both parageneses is sulfide (pentlandite, MSS or pyrrhotite). Earlier studies (Bulanova *et al.*, 1990) have shown that sulfide is the predominant inclusion type in Yakutian diamonds, as in diamonds worldwide. Sulfides would exist as melts or MSS crystals at the temperatures indicated for diamond growth by thermobarometry on diamond-inclusion silicates (900–1400°C; Griffin *et al.*, 1992, 1993). Several studies have proposed that sulfide melts could play a catalytic role in natural diamond nucleation, equivalent to that of the transition-metal melts used in the production of synthetic diamonds (Chepurov, 1988; Bulanova, 1995). The data presented here suggest that sulfides are part of a complex process that has introduced abundant incompatible elements into a generally depleted environment. The introduction of these elements requires another fluid phase, which may also have entrained droplets of an immiscible sulfide melt.

The apparent coexistence of diamond with both graphite and possible carbonate phases at the time of peridotitic diamond nucleation suggests a rapid transition of the carbon-bearing system from the precipitation of graphite $\pm$ carbonate to the stable crystallization of diamond. We suggest that the nucleation of diamond may have been induced by the introduction of a metasomatic fluid, probably accompanied by a thermal pulse (Griffin *et al.*, 1993). The temperatures recorded by many diamond-inclusion minerals are low enough (900–1100°C) that peridotitic host rocks would have been completely solid under vapour-absent conditions. The introduction of a complex fluid phase (including sulfide melts) may have lowered the solidus of the surrounding silicate rocks enough to produce local melting, providing a fluid in which diamond nucleated and grew. Alternatively, the introduced fluid itself may have been the medium from which the diamond nucleated and grew.

## Conclusions

(1) The mineral assemblages recorded in the central inclusions of Yakutian diamonds indicate nucleation in a reduced environment, with the oxygen fugacity controlled by the iron-wüstite equilibrium. The possible presence of carbonate suggests a transition toward the wüstite-magnetite buffer. (2) Nucleation of diamond occurred in the presence of a fluid, possibly a volatile-rich silicate melt, highly enriched in LIL and HFSE elements; this fluid also contained immiscible Fe-Ni-sulfide melts, and possibly immiscible carbonatitic melts, as components. (3) Nucleation of peridotitic diamonds occurred on a matrix of graphite+iron+wüstite, in an environment dominated by forsteritic olivine and Fe-Ni sulfide. (4) Nucleation of eclogitic diamonds occurred on a matrix of sulfide $\pm$ iron in an environment dominated by Fe-sulfide and omphacite ($\pm$K-Na-Al-Si melt).

## Acknowledgements

We thank John Cochrane for valuable assistance with the SEM analyses, and Ludmila Pavlova for help with EMP analysis. Alexsander Varshavskiy,who first identified the existence of the central inclusions in diamonds, inspired and encouraged this research and participated in its early stages. This is paper No. 104 from the ARC National Key Centre for Geochemical Evolution and Metallogeny of Continents (GEMOC).

## References

Bibby, D.M. (1979) Zonal distribution of impurities in diamond. *Geochim. Cosmochim. Acta*, **43**, 415–23.

Bulanova, G.P. (1995) The formation of diamond. *J. Geochem. Explor.*, **53**, 1–23.

Bulanova, G.P., Varshavskiy, A.V., Leskova, N.V. and Nikishova, L.V. (1979) On "central" inclusions in natural diamonds. *Doklady Akad. Nauk SSSR*, **244**, 704–6 (in Russian).

Bulanova, G.P., Novgorodov, P.G. and Pavlova, L.A. (1988) A first find of melt inclusions in diamond from Mir pipe. *Geokhimiya*, **5**, 756–65 (in Russian).

Bulanova, G.P., Spetsius, Z.V. and Leskova, N.V. (1990) *Sulfides in diamonds and mantle xenoliths from kimberlitic pipes of Yakutia*. Nauka, Novosibirsk, 118pp. (in Russian).

Bulanova, G.P. and Zayakina, N.V. (1991) Graphite-iron-cohenite assemblage in the central zone of diamond from 23rd Party Congress kimberlite. *Doklady Akad. Nauk SSSR*, **317**, 706–9 (in Russian).

Bulanova, G.P., Barashkov, Yu.P., Tal'nikova, S.B. and Smelova, G.B. (1993) *Natural diamond — genetic aspects*. Nauka, Novosibirsk, 176pp. (in Russian).

Bulanova, G.P., Griffin, W.L., Ryan, C.G., Shestakova, O.Ye. and Barnes, S.J. (1996) Trace elements in sulfide inclusions from Yakutian diamonds. *Contrib. Mineral. Petrol.*, **124**, 111–25.

Chepurov, A.J. (1988) On the role of sulfide melt in the process of diamond origin. *Geol. Geophys.*, **8**, 110–24 (in Russian).

Erasmus, C.S., Sellschop, J.P.F., Bibby, D.M., Fesq, H.W., Kable, E.J.D., Keddy, R.J., Hawkins, D.M., Mingay, D.W., Rasmussen, S.E., Renan, M.J. and Watterson, J.I.W. (1977) Natural diamonds — major, minor and trace impurities in relation to source and physical properties. *J. Radioanal. Chem.*, **38**, 133–46.

Griffin, W.L., Gurney, J.J. and Ryan, C.G. (1992) Variations in trapping temperatures and trace elements in peridotite-suite inclusions from African diamonds: evidence for two inclusion suites, and implications for lithosphere stratigraphy. *Contrib. Mineral. Petrol.*, **110**, 1–15.

Griffin, W.L., Sobolev, N.V., Ryan C.G., Pokhilenko, N.P, Win, T.T. and Yefimova, Y. (1993) Trace elements in garnets and chromites: diamond formation in the Siberian lithosphere. *Lithos*, **29**, 235–56.

Lambrecht, W.R.L., Lee, C.H., Segall, B., Angus, J.C., Li, Z. and Sunkara, M. (1993) Diamond nucleation by hydrogenation of the edges of graphitic precursors. *Nature*, **364**, 607–10.

Meyer, H.O.A. (1987) Inclusions in diamond. In *Mantle Xenoliths*. (P.H. Nixon, ed.), Wiley, pp. 501–22.

Milledge, H.J., Woods, P.A., Taylor, W.R., Bulanova, G.P. and Kaminsky, F.V. (1993) Cathodo-luminescence and infrared studies of Russian diamonds. Abstr. IAVCEI General Assembly, Canberra, 74.

Navon, O., Hutcheon, I.D., Rossman, G.R. and Wasserburg, G.L. (1988) Mantle-derived fluids in diamond micro-inclusions. *Nature*, **335**, 784–9.

Richardson, S.H., Gurney, J.J., Erlank, A.J. and Harris, J.W. (1984) Origin of diamond in old enriched mantle. *Nature*, **310**, 198–202.

Ryan, C.G., Cousens, D.R., Heinrich, C.A., Griffin, W.L., Sie, S.H. and Mernagh, T.P. (1991) Quantitative PIXE microanalysis of fluid inclusions, based on a layered yield model. *Nucl. Instr. Meth.*, **B54**, 292–7.

Schrauder, M. and Navon, O. (1994) Hydrous and carbonatic mantle fluids in fibrous diamonds from Jwaneng, Botswana. *Geochim. Cosmochim. Acta*, **58**, 761–71.

Schrauder, M., Navon, O. and Harris, J.W. (1993) Carbonate and water-bearing fluids trapped in an octahedral peridotitic diamond. *EOS, Trans. Amer. Geophys. Union*, **74**, 636.

Schrauder, M., Koeberl, C. and Navon, O. (1996) Trace element analyses of fluid-bearing diamonds from Jwaneng, Botswana. *Geochim. Cosmochim. Acta*, **60**, 4711–24.

Sunagawa, I. (1984) Morphology of natural and synthetic diamond crystals. In *Material Science of the Earth's Interior*. (I. Sunagawa, ed.) Terrapub., Tokyo, pp. 303–31.

Varshavskiy, A.V. (1968) *Anomalous birefringence and internal morphology of diamonds*. Nauka, Moscow, 89 pp. (in Russian).

[*Manuscript received 12 August 1997: revised 28 November 1997*]